2021

Evaluation of Anisotropic Magnetoresistive (AMR) Sensors for a Magnetic Field Scanning System for SRF Cavities

Ishwari P. Parajuli
Old Dominion University, ipara001@odu.edu

Gianluigi Ciovati
Old Dominion University, gciovati@odu.edu

Jean R. Delayen
Old Dominion University, jdelayen@odu.edu

Alex V. Gurevich
Old Dominion University, agurevic@odu.edu

Liu Lin (Ed.)

See next page for additional authors

Original Publication Citation

Parajuli, I. P., Ciovati, G., Delayen, J. R., & Gurevich, A. V. (2021). Evaluation of anisotropic magnetoresistive (AMR) sensors for a magnetic field scanning system for SRF cavities. In L. Lin, J.M. Byrd, R. Neuenschwander, R. Picoreti, & V.R.W. Schaa, (Eds.), *Proceedings of the 12th International Particle Accelerator Conference* (pp. 2304-2307). Joint Accelerator Conferences Website. https://doi.org/10.18429/JACoW-IPAC2021-TUPAB344

ISBN: 978-3-95450-214-1 ISSN: 2673-5490 doi:10.18429/JACoW-IPAC2021-TUPAB344

EVALUATION OF ANISOTROPIC MAGNETORESISTIVE (AMR) SENSORS FOR A MAGNETIC FIELD SCANNING SYSTEM FOR SRF CAVITIES*

I. Parajuli†, G. Ciovati[1], J. Delayen, and A. Gurevich
Center for Accelerator Science, Physics Department, Old Dominion University, Norfolk, VA 23529, USA
[1]also at Jefferson Lab, Newport News, VA 23606, USA

Abstract

One of the significant causes of residual losses in superconducting radio-frequency (SRF) cavities is trapped magnetic flux. The flux trapping mechanism depends on many factors that include cool-down conditions, surface preparation techniques, and ambient magnetic field orientation. Suitable diagnostic tools are not yet available to quantitatively correlate such factors' effect on the flux trapping mechanism. A magnetic field scanning system (MFSS) utilizing anisotropic magnetoresitive sensors, fluxgate magnetometers, or Hall probes was recently commissioned to scan the local magnetic field of trapped vortices around 1.3 GHz single-cell SRF cavities. In this contribution, we will present results from sensitivity calibration and the first tests of AMR sensors in the MFSS.

INTRODUCTION

Superconducting Radio-frequency (SRF) cavities are fundamental building blocks of modern particle accelerators. Bulk niobium is a material of choice to fabricate SRF cavities. Due to the extensive research and development on niobium cavities, their performance is getting better. One of the sources of power dissipation on SRF cavities is residual losses. Several experiments show that trapped flux is one of the causes of the residual losses in SRF cavities [1, 2]. Cooling Nb cavities with higher temperature gradient at Tc results in less amount of trapped magnetic flux get, whereas cooling the cavity at smaller temperature gradients ($\Delta T < 200$ mK) results in most of the residual magnetic field getting trapped within the superconductor. Flux trap mechanism also depends on the material preparation [2, 3]. However, there are several unknowns about the trapped flux. For example; what is the distribution of trapped flux on the cavity surface? How much magnetic flux gets trapped at a particular location? How this trapped flux behaves with high rf field? A magnetic field scanning system (MFSS) consisting of Hall Probes and Fluxgate magnetometers has been designed, built and commissioned [4]. An alternative magnetic field sensor which could be used to measure the trapped flux on the surface of SRF cavity is an anisotropic magnetoresistive (AMR) sensor. In references [5, 6] authors showed that AMR sensors are suitable to work at cryogenic temperature and suitable for the trapped flux measurement. In this work, we have calibrated 16 AMR sensors. We used four of the calibrated sensors in the MFSS. We were able to detect the change in the local magnetic field resulting from the transition from normal conducting to superconducting state and the amount of trapped flux around the cavity surface.

AMR SENSOR

Anisotropic magneto-resistive effect is a quantum mechanical effect whose origin lies on the combined action of magnetization and spin orbit interaction. If we keep the ferromagnetic material in an external magnetic field its resistance changed. This change in resistance of ferromagnetic material upon application of magnetic effect is called AMR effect. The change in resistance depends on the direction of the applied current and magnetization direction of the material. Anisotropic magneto-resistive effect in nickel and iron was first observed by W. Thomson in 1857 [7]. Each AMR sensor consists of four AMR elements in a Wheatstone bridge configuration.

AMR elements are built in barberpole structure so that the direction of the applied magnetic field can be identified. A commercial AMR sensor (Sensitec, AFF755B), which has already been used for magnetic field studies of SRF cavities [5] was considered in this study. A schematic detail of AMR sensor is shown in Fig. 1. The single-axis AMR sensors also have a flip coil and a test coil. To initialize the magnetization of AMR elements in one direction, the flip coil can be used. The test coil can be used to test the performance of AMR sensor.

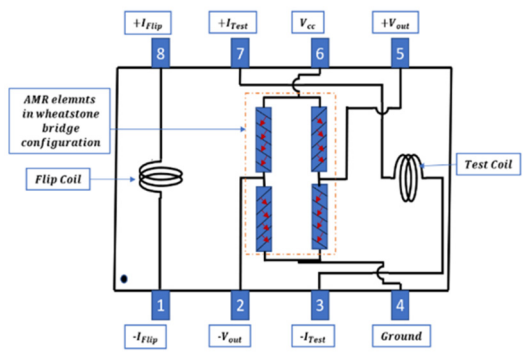

Figure 1: Schematic diagram of AMR sensor.

*Work supported by NSF Grant 100614-010. Jefferson lab work is supported by Jefferson Science Associates, LLC under U.S. DOE Contract No. DE-AC05-06OR23177.
† ipara001@odu.edu

ISBN: 978-3-95450-214-1 ISSN: 2673-5490 doi:10.18429/JACoW-IPAC2021-TUPAB344

EXPERIMENTAL STEUP AND EXPERIMENTAL PROCEDURE

AMR sensor calibration setup consists of Helmholtz coils, a printed circuit board, liquid helium Dewar, a single axis fluxgate magnetometer, a Mag01-H, a pulse current source, a direct current source, and a digital multi-meter. Figure 2 shows the schematic diagram of the calibration setup.

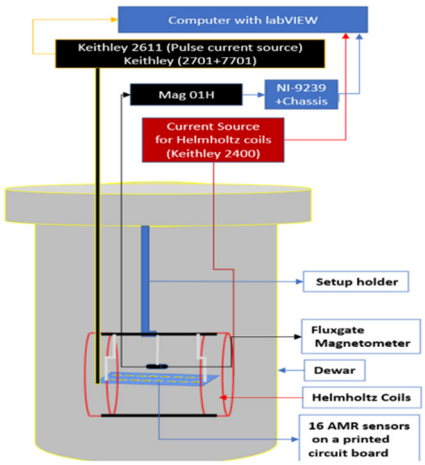

Figure 2: Schematic diagram of AMR sensor calibration setup.

Calibration was done in the following steps:

1. Initially, we kept the external magnetic field as low as possible (B_{ext} ~1 mG).
2. We cooled the sensors at desired temperature by keeping them in liquid helium dewar.
3. We applied 150 mA of positive pulse current of pulse width 200 µs to initialize the magnetization of the AMR sensor.
4. We measured the voltage and take that voltage as offset voltage (V_{offset}).
5. We increased the external magnetic field by ΔB_{ext} and measured the voltages (V_{amr}) from each AMR sensors, and we also measured the applied external magnetic field.
6. We repeated step (5).

After calibration was done, we plotted the $V=|V_{amr}-V_{offset}|$ vs. B_{ext}. The slope of that plot gave sensitivity of AMR sensors. After calibration, we installed four AMR sensors in the magnetic field scanning system, in such a way to measure the magnetic field component normal to the cavity surface. More detail about the magnetic field scanning system can be found in reference [4]. Figure 3 shows the schematic diagram of MFSS with AMR sensors. Figure 4 (a) shows the photo of MFSS attached in a single cell 1.3 GHz niobium cavity, and Fig. 4 (b) shows a enlarged image of four AMR sensors in a bracket. To test the performance of the AMR sensors we did several experiments. In first experiment, we applied the external magnetic field of ~100 mG along the cavity axis and we measured the applied field using three fluxgatemagnetometer. After that we did fast cool-down through T_c. During fast cool-down we measured the magnetic field using four AMR sensors. During first test, all AMR sensors were kept at fixed locations. In another experiment we applied the external magnetic field of ~100 mG along cavity axis at temperature $T>T_c$, we performed a slow cool-down through T_c. Once the temperature of the cavity reached below T_c we decreased the external magnetic field to ~1 mG, after that we performed the magnetic field scanning around the cavity surface in the following ways. First, we kept the sensors at $\alpha=0^o$ azimuthal position and we measured the magnetic field at that particular position. After that we increased the azimuthal angle by $\Delta\alpha=10^o$ and again measured the magnetic field. We repeated these steps until we reached $\alpha=360^o$ azimuthal position.

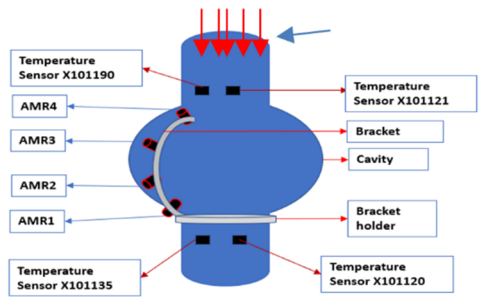

Figure 3: Schematic diagram of MFSS with four AMR sensors.

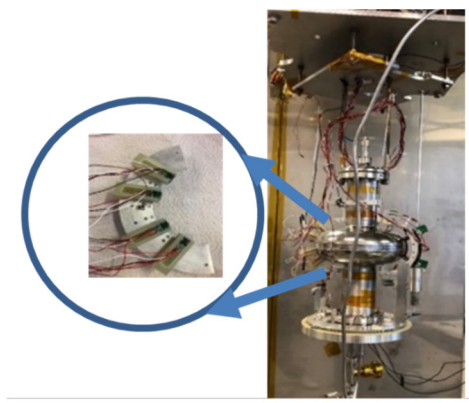

Figure 4: (a) MFSS with AMR sensors in 1.3 GHz Tesla shape single cell cavity, and (b) four AMR sensors in a bracket.

RESULTS AND DISCUSSION

Figure 5 shows the offset voltage versus temperature of sixteen AMR sensors at different temperatures. Average offset voltage at four different temperature for 16 sensors is 1.25±0.47 mV. Figure 6 shows the sensitivity versus temperature of all 16 AMR sensors. The average sensitivity of all 16 sensors is ~178 µV/µT. The standard deviation of sensitivities at particular temperature is within 2%. Figure 7 shows the magnetic field measured by four AMR sensors versus time and temperature vs time during fast cool-down. The external magnetic field during fast cool-down was ~100 mG. Since AMR1 and AMR4 were at 35º with respect to the cavity axis, and AMR2 and AMR3 were

ISBN: 978-3-95450-214-1 ISSN: 2673-5490 doi:10.18429/JACoW-IPAC2021-TUPAB344

at 66.4° with respect to the cavity axis, the magnitude of magnetic field measured was different. From this plot it is also clear that magnetic flux density decreased at the field along a parallel of each AMR sensors. AMR4 was near the upper beam tube, and was tilted by 35° with respect the cavity axis. Similarly, AMR1 was near the bottom beam tube, and was tilted by 35° with respect to cavity axis. Since, we had applied ~100 mG external magnetic field during slow cool down, the maximum field that could have been trapped at the parallels of AMR1 and AMR4 is cos35°×100 mG ~82 mG. From Fig. 8 it is clear that at parallels of AMR1 and AMR4 almost 100% of applied magnetic field was trapped during slow cool-down. Similarly the AMR2 was located just below the equator and had 66.4° with respect the cavity axis, and AMR3 was located just above the equator and had 66.4° angle with respective to the cavity axis. At the corresponding parallel of AMR2 and AMR3 the ideal trap flux amount would be cos66.4°×100 mG ~40 mG. However, from measurement it was observed that around 25 mG of field had trapped.

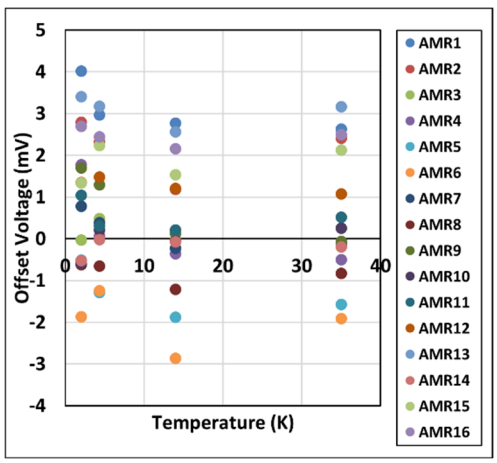

Figure 5: Offset voltage vs. temperature.

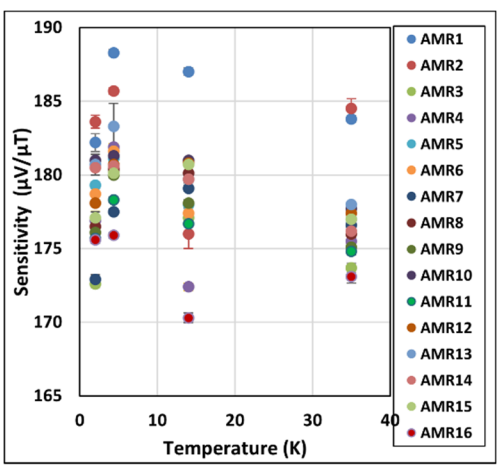

Figure 6: Sensitivity vs. temperature.

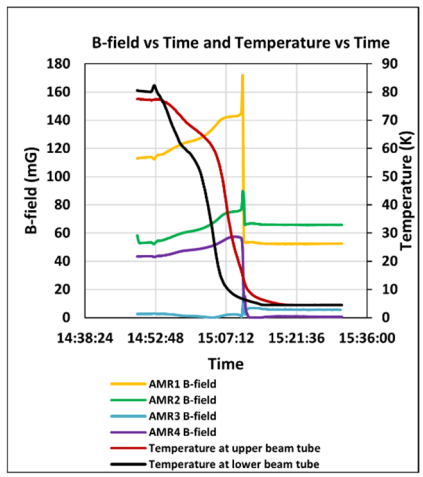

Figure 7: Magnetic field vs. time and temperature vs. time.

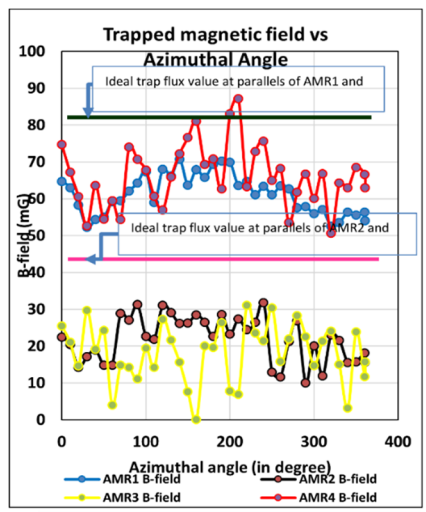

Figure 8: Trapped magnetic field vs. azimuthal.

SUMMARY AND OUTLOOK

We have successfully calibrated 16 AMR sensors at four different temperatures. The average sensitivity of all sensors is 178 μV/μT. The standard deviation of the sensitivities at a particular temperature is within ~2%. The offset voltages of AMR sensors at different temperatures is different. The variation could be up to 35% i.e., offset voltage heavily depend on temperature. AMR sensors installed on a MFSS were able to detect the superconducting transition of niobium cavity and to measure the trapped flux around the niobium cavity surface. The amount of the trapped flux on the cavity surface was not uniform. At parallels of AMR1 and AMR4 almost 100% flux got trapped whereas at parallels of AMR2 and AMR3 only 60% of magnetic flux got trapped.

In future we are planning to install AMR sensors in final setup of MFSS. Also, we are planning to build a combined magnetic and temperature mapping system for 3 GHz cavities using both AMR sensors and temperature sensors.

ACKNOWLEDGEMENTS

We would like to thank for the technical support by the SRF staff and the machine shop staff at Jefferson Lab.

ISBN: 978-3-95450-214-1 ISSN: 2673-5490 doi:10.18429/JACoW-IPAC2021-TUPAB344

REFERENCES

[1] C. Vallet et al., "Flux Trapping in Superconducting Cavities", in *Proc. 3rd European Particle Accelerator Conf. (EPAC'92)*, Berlin, Germany, Mar. 1992, pp. 1295-1298.

[2] H. Padamsee, J. Knobloch, and T. Hays, *RF Superconductivity for Accelerators*. New York, USA: Wiley & Sons, 1998.

[3] A. Romanenko, A. Grassellino, O. Melnychuk, and D. A. Sergatskov, " Dependence of the residual surface resistance of superconducting radio frequency cavities on the cooling dynamics around T_c", *J. Appl. Phys.*, vol. 115, p. 184903, 2014. doi:10.1063/1.4875655

[4] I. P. Parajuli, G. Ciovati, W. A. Clemens, J. R. Delayen, A. V. Gurevich, and J. Nice, "Design and Commissioning of a Magnetic Field Scanning System for SRF Cavities", in *Proc. 19th Int. Conf. RF Superconductivity (SRF'19)*, Dresden, Germany, Jun.-Jul. 2019, pp. 547-549. doi:10.18429/JACoW-SRF2019-TUP052

[5] B. Schmitz, J. Köszegi, K. Alomari, O. Kugeler, and J. Knobloch, "Magnetometric mapping of superconducting RF cavities", *Review of Scientific Instruments*, vol. 89, no. 5, p. 054706, 2018. doi:10.1063/1.5030509

[6] T. Okada *et al.*, "Systematic evaluation of magnetic sensitivities of anisotropic magnetoresistive sensors at liquid helium temperature for superconducting cavities", *Review of Scientific Instruments*, vol. 92, no. 3, p. 035003, 2021. doi:10.1063/5.0038805

[7] W. Thomson, "On the electro-dynamic qualities of metals: Effects of magnetization on the electric conductivity of nickel and of iron," *Proceedings of the Royal Society of London*, vol. 8, pp. 546-550, 1857. doi:10.1098/rspl.1856.0144